Am J Physiol Heart Circ Physiol 293: H2409–H2417, 2007.
First published July 13, 2007; doi:10.1152/ajpheart.00562.2007.

Phosphorylation of RyR_2 and shortening of RyR_2 cluster spacing in spontaneously hypertensive rat with heart failure

Ye Chen-Izu,[1] Christopher W. Ward,[2] Wayne Stark Jr.,[3] Tamas Banyasz,[1,4] Marius P. Sumandea,[1] C. William Balke,[1] Leighton T. Izu,[1] and Xander H. T. Wehrens[5]

[1]*Departments of Internal Medicine and Physiology, University of Kentucky College of Medicine, Lexington, Kentucky;* [2]*School of Nursing and* [3]*School of Medicine, University of Maryland, Baltimore, Maryland;* [4]*Department of Physiology, University Medical School of Debrecen, Debrecen, Hungary; and* [5]*Departments of Molecular Physiology and Biophysics, and Medicine (Cardiology), Baylor College of Medicine, Houston, Texas*

Submitted 14 May 2007; accepted in final form 11 July 2007

Chen-Izu Y, Ward CW, Stark Jr. W, Banyasz T, Sumandea MP, Balke CW, Izu LT, Wehrens XH. Phosphorylation of RyR_2 and shortening of RyR_2 cluster spacing in spontaneously hypertensive rat with heart failure. *Am J Physiol Heart Circ Physiol* 293: H2409–H2417, 2007. First published July 13, 2007; doi:10.1152/ajpheart.00562.2007.—As a critical step toward understanding the role of abnormal intracellular Ca^{2+} release via the ryanodine receptor (RyR_2) during the development of hypertension-induced cardiac hypertrophy and heart failure, this study examines two questions: *1*) At what stage, if ever, in the development of hypertrophy and heart failure is RyR_2 hyperphosphorylated at Ser^{2808}? *2*) Does the spatial distribution of RyR_2 clusters change in failing hearts? Using a newly developed semiquantitative immunohistochemistry method and Western blotting, we measured phosphorylation of RyR_2 at Ser^{2808} in the spontaneously hypertensive rat (SHR) at four distinct disease stages. A major finding is that hyperphosphorylation of RyR_2 at Ser^{2808} occurred only at late-stage heart failure in SHR, but not in age-matched controls. Furthermore, the spacing between RyR_2 clusters was shortened in failing hearts, as predicted by quantitative model simulation to increase spontaneous Ca^{2+} wave generation and arrhythmias.

ryanodine receptor; hypertension; cardiac hypertrophy; protein kinase A; spontaneously hypertensive rat

DURING THE DEVELOPMENT of hypertensive heart disease, heart failure (HF) is often preceded by concentric cardiac hypertrophy (11). Although the molecular mechanisms of this transition are incompletely understood (9), defects in excitation-contraction (E-C) coupling are thought to play a central role in cardiac hypertrophy and HF (12, 43). In HF, increased phosphorylation of ryanodine receptors (RyR_2) at Ser^{2808} (RyR_2-Ser^{2808}) has been proposed to enhance RyR_2 channel sensitivity to cytosolic Ca^{2+} concentration, resulting in Ca^{2+} leakage from the sarcoplasmic reticulum (SR) and, thus, reduction of the SR Ca^{2+} load (23, 24). Reduced SR Ca^{2+} load is expected to decrease E-C coupling gain, leading to depressed myocardial contractility and pump failure (3, 40). However, the concept that RyR_2-Ser^{2808} is hyperphosphorylated in failing hearts has been a subject of debate in the literature.

Hyperphosphorylation of RyR_2 channels at Ser^{2808} in failing hearts has been reported in multiple clinical and experimental studies (1, 23, 31, 42, 45). However, other studies reported no obvious change in RyR_2-Ser^{2808} phosphorylation in some animal models of HF (15, 48). The discrepancy could be due to differences in the etiology or the severity of heart disease in different models. It has become clear that a better understanding of the temporal profile of RyR_2-Ser^{2808} phosphorylation during the progressive development of cardiac hypertrophy and HF is warranted to resolve this controversy. Therefore, we carefully examined the phosphorylation level of RyR_2-Ser^{2808} at various stages of hypertensive heart disease from the development of cardiac hypertrophy to HF. Moreover, we measured changes in RyR_2-Ser^{2808} phosphorylation in different regions of the heart, inasmuch as regional heterogeneity in Ca^{2+}-handling proteins might also affect cardiac contractility.

It has been proposed that defects in E-C coupling in HF may result not only from dysregulation of Ca^{2+}-handling proteins, but also from restructuring of the spatial organization of RyR_2 clusters that form Ca^{2+} release units (CRUs) within the cardiomyocyte (7, 14). Although changes in CRU organization are expected to affect the Ca^{2+} dynamics, such changes have yet to be demonstrated in HF. Also unknown is the correlation between the spatial organization and the modulation (i.e., PKA phosphorylation levels) of RyR_2 in heart disease development.

The progression of concentric hypertrophy to HF has been well demonstrated in the spontaneously hypertensive rat (SHR) model, which mimics human essential hypertension and heart disease (4). We hypothesized that in the SHR model the transition from cardiac hypertrophy to HF might influence the level of RyR_2 phosphorylation, as well as the subcellular organization of CRUs. The purpose of this study is to determine whether the progressive development of hypertensive heart disease in SHR is accompanied by *1*) changes in the phosphorylation of RyR_2-Ser^{2808} and *2*) changes in the spatial distribution of CRUs in ventricular myocytes.

MATERIALS AND METHODS

Animals and tissue preparation. Male SHR, normotensive Wistar-Kyoto rats (WKY), and Sprague-Dawley rats were purchased from Charles River (http://www.criver.com). Blood pressure was monitored weekly in nonanesthetized SHR and WKY by the tail-cuff method. For tissue preparation, rats were anesthetized with pentobarbital sodium (100 mg/kg ip with 4,000 U/kg heparin). Isoproterenol (1 mg/kg ip) was injected before cardiac explantation for the β-adrenergic receptor stimulation experiments. After suppression of spinal cord reflexes, the heart was exposed via a midline thoracotomy, and

Address for reprint requests and other correspondence: Y. Chen-Izu, Dept. of Internal Medicine, Univ. of Kentucky College of Medicine, 741 S. Limestone St., BBSRB, Rm. B255, Lexington, KY 40536-0509 (e-mail: YeChen-Izu@uky.edu).

The costs of publication of this article were defrayed in part by the payment of page charges. The article must therefore be hereby marked "*advertisement*" in accordance with 18 U.S.C. Section 1734 solely to indicate this fact.

the chambers were rinsed with Ca^{2+}-free PBS, which was injected into the left ventricle (LV) and vented through a small incision in the right atrial free wall. The heart was subsequently removed, and laterally dissected to expose the ventricular walls and chambers. Tissue freezing medium (OCT compound) was injected into the chambers to preserve cardiac morphology during the subsequent freezing process. The tissue was flash frozen by submersion in chilled isopentane for 10–20 s, placed on dry ice, and then stored in a −80°C freezer. The frozen tissue was cut into 20-μm-thick sections in a cryostat (model 2800 Frigocut-E, Reichert, Bannockburn, IL). All chemicals and reagents were purchased from Sigma-Aldrich if not specified otherwise. All animals were handled strictly in accordance to the National Institutes of Health guidelines and protocols approved by our Institutional Animal Care and Use Committee at the University of Kentucky.

Western blot. Western blot was used to measure the amount of phosphorylation of RyR_2-Ser^{2808} relative to the total amount of RyR_2 in LV tissue according to a previously published protocol (32). Phosphorylated RyR_2-Ser^{2808} (RyR_2-pSer^{2808}) was stained using a phosphorylated epitope-specific antibody [affinity-purified polyclonal rabbit antibody raised against phosphorylated peptide sequence C-RTRRI-(pS)-QTSQV]; total RyR_2 was stained using a polyclonal anti-RyR_2 antibody.

Semiquantitative immunohistochemistry. Tissue sections were incubated in a blocking solution containing 5% goat serum and 3% BSA in PBS for 30 min and rinsed twice in PBS; then the sections were incubated in primary antibody solution (1:200 dilution) for 1.5 h, rinsed twice in PBS, and incubated in secondary antibody solution (1:200 dilution) for 1.5 h. The same phosphorylated epitope-specific (polyclonal, rabbit) antibody was used in semiquantitative immunohistochemistry (SQ-IHC) and quantitative Western blot to label RyR_2-pSer^{2808}, and a monoclonal pan anti-RyR_2 antibody (mouse IgG1; clone C3-33, Affinity BioReagents) was used to label total RyR_2 in SQ-IHC. Phosphorylated and pan RyR_2 labeling were visualized using secondary antibody-conjugated fluorophores: anti-rabbit IgG-conjugated Alexa Fluor 569 and anti-mouse IgG-conjugated Alexa Fluor 488, respectively. The antibody-labeled tissue sections were covered with Antifade and sealed under a glass coverslip (no. 1) for imaging.

Confocal imaging and image analysis for SQ-IHC. Confocal images were obtained using a confocal microscope (Radiance 2000, Bio-Rad) with a water immersion objective (×63, NA 1.2) corrected for the thickness of the no. 1 glass coverslip. To obtain confocal images of antibody labeling, we placed the focal plane in the middle of the 20-μm-thick tissue slice to avoid the interface between the tissue and the glass. The imaging areas were chosen by random scanning of the tissue section, and various areas in the tissue section were used to obtain an average value. For quantitative analysis and comparison between the control group and the test group, we strictly used identical antibody labeling conditions and confocal imaging parameters for all the tissue samples in the groups of comparison.

To quantitatively measure the labeling intensity, we recorded the fluorescence emission from a defined area (using a ×63 objective and 1,024 × 1,024 pixels in the *x*-*y* plane) with a defined depth (pinhole size optimized to confocal *z* resolution of ~1 μm). Histograms of the optical intensity [i.e., fluorescence intensity (FI)] of each pixel were plotted. The background signal was subtracted from the total histogram before the average FI was calculated. The average FI was then calculated for each image. To calculate the relative phosphorylation of RyR_2-Ser^{2808}, we double labeled RyR_2-Ser^{2808} and the total RyR_2 in the tissue using specific primary antibodies and secondary antibody-conjugated Alexa Fluor 568 and Alexa Fluor 488, respectively. The ratio of the average FI of Alexa 568 to that of Alexa 488 reflects the amount of RyR_2-Ser^{2808} relative to the total amount of RyR_2.

The images used to calculate the antibody labeling intensity were obtained without digital zoom (gain = 1), and the images used to measure the spacing between RyR_2 clusters (CRUs) were obtained with maximum digital zoom (gain = 10). The spacing between RyR_2 clusters along the longitudinal axis of the cells was measured using our previously described method (7).

Cell isolation. The rats were anesthetized with pentobarbital sodium (Nembutal; 100 mg/kg ip). Hearts were tested for the suppression of reflexes and then explanted via a midline thoracotomy. A standard enzymatic technique was used to isolate the ventricular myocyte. Briefly, the heart was mounted on a Langendorff system and perfused with a modified Tyrode solution containing (in mmol/l) 135 NaCl, 4 KCl, 1.0 $MgSO_4$, 0.34 NaH_2PO_4, 15 glucose, 10 HEPES, and 10 taurine, with pH adjusted to 7.25 with NaOH; the perfusion solution was prewarmed to 37°C and bubbled with 100% O_2. Then collagenase B (~1 mg/ml; Hoffmann-La Roche, Basel, Switzerland), protease type XIV (~0.1 mg/ml), 0.1% BSA, and 20 μM Ca^{2+} were added into the perfusion solution, and the heart was enzymatically digested for 15–20 min. The ventricular tissue was cut down and minced, the remaining tissue was further incubated in the enzyme solution at 37°C for 15–45 min and minced again, and the ventricular myocytes were collected.

Immunocytochemistry. Freshly isolated ventricular myocytes were labeled using anti-RyR_2 monoclonal antibody (mouse IgG1; clone C3-33, Affinity BioReagents) as described preciously in detail (7, 14).

Statistical analysis. All samples were coded using randomized codes for blinded processing during experiments and data analysis. Values are means ± SD. Unpaired Student's *t*-test with equal variance and two tails was used to compare the age-matched SHR vs. WKY; the difference in the mean values is deemed significant if $P < 0.05$. Two-way ANOVA was used to evaluate the differences in the longitudinal study of the age-related changes in WKY and in the disease-related changes in SHR.

RESULTS

Progressive development of hypertrophy and HF in SHR. Hypertensive heart disease develops progressively in SHR through distinctive stages of hypertension, cardiac hypertrophy, and HF. The history of blood pressure development is shown in Fig. 1*A*. SHR were prehypertensive during their first 4–6 wk of life, rapidly developed hypertension at 8–12 wk of age, and remained hypertensive thereafter. In comparison, WKY controls remained normotensive throughout their ~2-yr life span. After the onset of hypertension, cardiac hypertrophy gradually developed in SHR at 3–18 mo of age, and HF typically occurred at 1.5–2 yr of age. The history of hypertrophy development in SHR is shown in Fig. 1*B*. As a normotensive control, WKY displayed a slight decrease in heart weight-to-body weight ratio (HW/BW), as the increase in body weight outpaced the increase in heart weight as the animals aged. HW/BW was the same in 5-wk-old (prehypertensive) and 11-wk-old (onset of hypertension) SHR as in age-matched WKY controls. HW/BW was significantly higher in 1-yr-old SHR than in age-matched WKY, demonstrating cardiac hypertrophy: 5.38 ± 0.77 ($n = 10$) vs. 3.84 ± 0.51 (SD) mg/g ($n = 7$; $P < 0.05$, *t*-test). During HF, HW/BW was higher in SHR than in age-matched WKY [6.19 ± 1.68 ($n = 5$) vs. 3.63 ± 1.13 mg/g ($n = 18$)], but the individual variation was greater during HF, most likely due to cardiac cachexia ($P < 0.1$, *t*-test). Consistent with previous studies showing echocardiographic evidence for HF in >1.5-yr-old SHR (6, 8, 34, 35), we found clinical signs of HF (e.g., severe hypertrophy or chamber dilation, ascites, pericardial effusion, chest edema, and lung edema) in SHR at postmortem examination.

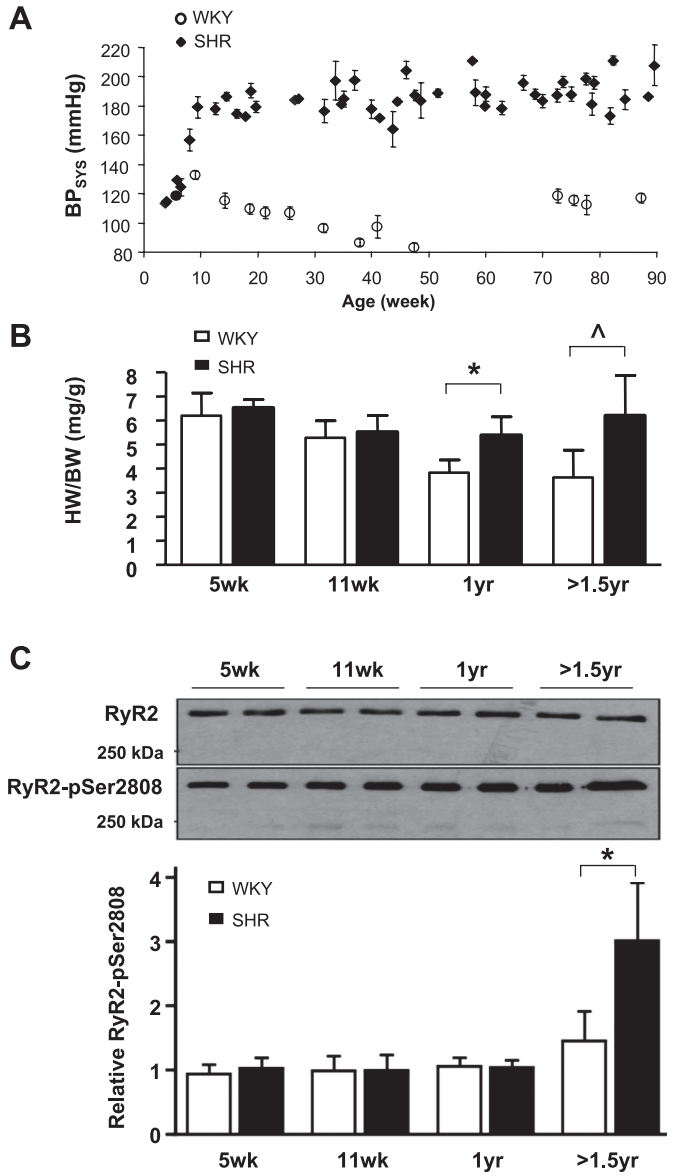

Fig. 1. Progressive development of hypertrophy and heart failure (HF) in spontaneously hypertensive rats (SHR). *A*: systolic blood pressure (BP_{sys}) in SHR ($n > 20$) and Wistar-Kyoto rats (WKY, $n > 20$). SHR developed hypertension starting at 6–12 wk of age; WKY controls remained normotensive throughout ~2 yr of life span. *B*: age-dependent heart weight-to-body weight ratio (HW/BW) in SHR and WKY. $*P < 0.05$; $\wedge P < 0.1$ (Student's *t*-test). *C*: Western blot analysis (*top*) and quantitative measurement (*bottom*; $n = 4$ animal/group) of phosphorylation of ryanodine receptor at Ser^{2808} (RyR_2-Ser^{2808}) in left ventricle (LV). Relative level of RyR_2-Ser^{2808} phosphorylation (RyR_2-$pSer^{2808}$) remained normal in the first 3 stages of hypertensive heart disease development but drastically increased at end-stage HF. $*P < 0.05$ (*t*-test). Two-way ANOVA shows significant differences between strains ($P = 0.007$), between ages ($P < 0.0001$), and in interaction ($P = 0.001$); Bonferroni's posttest shows significant difference between SHR >1.5 yr and WKY >1.5 yr ($P < 0.001$).

Western blot measurement of RyR_2-$pSer^{2808}$ phosphorylation. We used the standard Western blot technique to measure RyR_2-$pSer^{2808}$. Figure 1*C* shows Western blot measurement of RyR_2-$pSer^{2808}$ relative to total RyR_2 in the LV of SHR at four distinct disease stages: 5-wk-old prehypertensive SHR, 11-wk-old SHR after the onset of hypertension but before hypertrophy, 1-yr-old SHR with overt hypertrophy, and >1.5-yr-old SHR at HF. The results show that RyR_2-Ser^{2808} phosphorylation drastically increased in >1.5-yr-old SHR [3.00 ± 0.94 in SHR vs. 1.44 ± 0.49 in WKY ($n = 4$, $P < 0.05$ by *t*-test and $P < 0.001$ by 2-way ANOVA with Bonferroni's posttest)] after the progression from hypertrophy to HF.

SQ-IHC method development. To provide another independent measure for RyR_2-Ser^{2808} phosphorylation levels, we developed an SQ-IHC method by combining immunohistochemistry and confocal microscopy techniques (Fig. 2*A*). The specificity of antibody labeling was verified by preincubation of the antibody with its phosphorylated epitope peptide, which also served as the background image for subtraction of the nonspecific labeling. Basal RyR_2-$pSer^{2808}$ in the control tissue was relatively low (Fig. 2*B*). In contrast, intense labeling of RyR_2-$pSer^{2808}$ was observed in cardiac tissue obtained from the heart pretreated with isoproterenol, which induced PKA phosphorylation of RyR_2 due to β-adrenergic stimulation (Fig. 2*B*). The punctate staining in a striated pattern is also consistent with the known RyR_2 clustering and localization on Z disks (7).

The original SQ-IHC method used a digital camera to image and quantify the molecules in tissue samples (25). We improved on the original SQ-IHC method by employing confocal microscopy to image optical sections inside the tissue (avoiding tissue surface artifacts) and strictly controlled the amount of fluorescence emission by using a fixed area and a fixed depth in the optical section [providing normalization for averaging across different sections, so the labeling intensity in each image is measured from a unit volume (normalized) and, hence, can be used to compare different tissue sections]. FI values of all pixels in a representative image are shown in Fig. 2*C*. The background image showed very low (<34) FI, in accordance with low background labeling. The antibody labeling image showed well-distributed FI values across the digitizing range for intensity without saturation. To subtract the background, we truncated the FI histogram of each image by removing all points <34 FI. This subtraction also digitally removed "holes" in the tissue section caused by physiological structures (e.g., capillary, nerve, and extracellular space). The mean FI of each image was then calculated from the background-subtracted histogram. We used identical treatment for all tissue samples throughout the process, from antibody labeling (reagents and protocol) to confocal imaging (optical and parameter settings), to eliminate variations.

To measure the RyR_2-$pSer^{2808}$ relative to the total amount of RyR_2 protein in a tissue section, we double labeled sections using a phosphorylated epitope-specific antibody recognizing RyR_2-$pSer^{2808}$ and a pan RyR_2 antibody tagged with secondary antibody-conjugated Alexa Fluor 568 and Alexa Fluor 488, respectively (Fig. 2*D*, pseudocolored red for RyR_2-$pSer^{2808}$ and green for pan RyR_2). The SQ-IHC method was used to obtain mean FI values for each antibody labeling; then we calculated the ratio of mean FI values of RyR_2-$pSer^{2808}$ to the total RyR_2 labeling, which provided a measure for the relative amount of RyR_2-$pSer^{2808}$ in the tissue. A great benefit of this ratiometric method is that it eliminates the variations in different tissue regions (e.g., cell density, orientation, and accessibility) and, hence, enables us to average across different tissue sections. The ratiometric method was used to measure relative RyR_2-$pSer^{2808}$ in control and epinephrine-treated hearts, and the results are shown in Fig. 2*E*. Infusion of epinephrine into

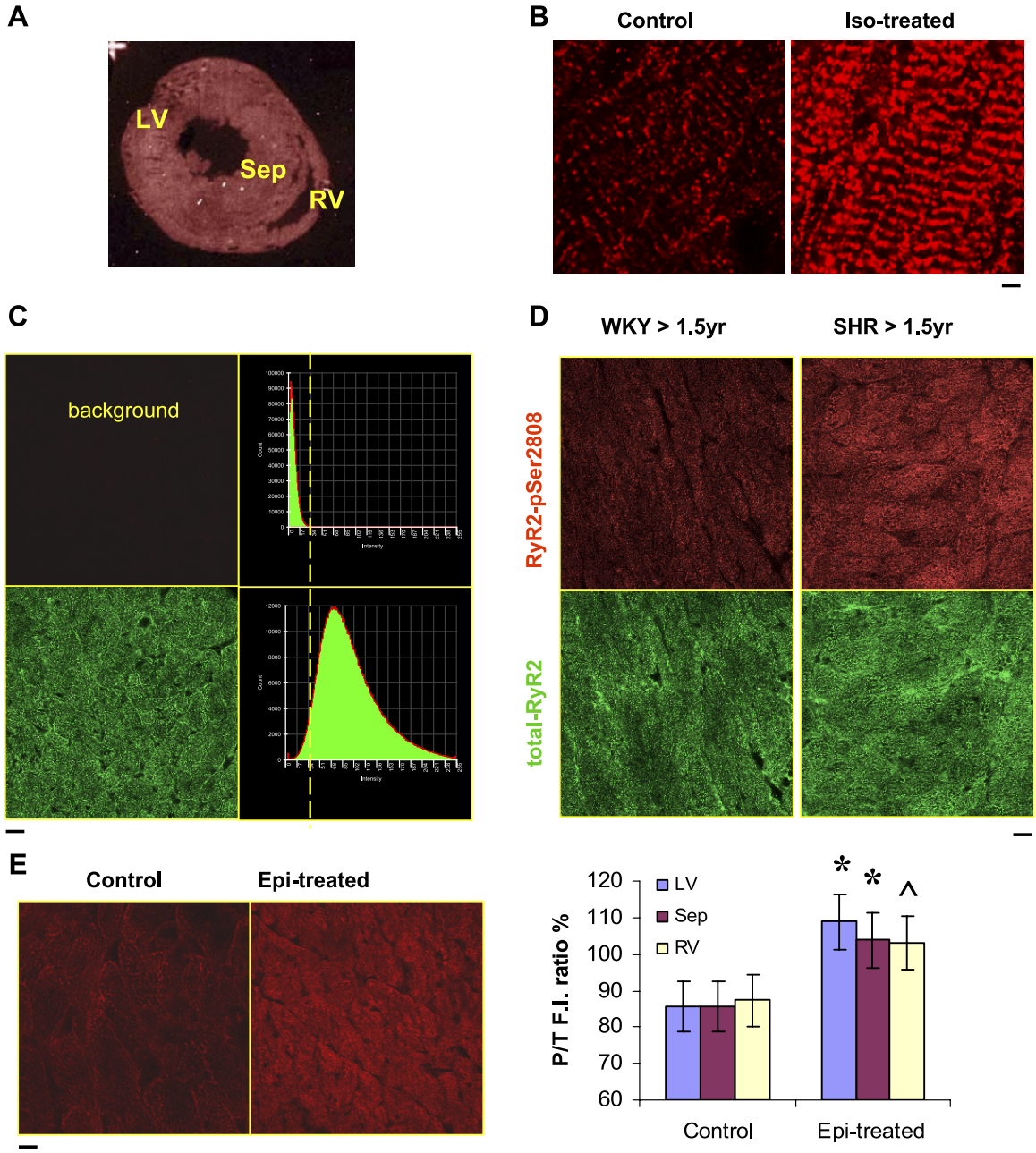

Fig. 2. Quantitative immunohistochemistry methodology. *A*: representative 20-μm-thick tissue cross section from frozen rat heart. RyR_2-$pSer^{2808}$ in tissue was labeled using a phosphorylated epitope-specific antibody and visualized using the secondary antibody-conjugated Alexa Fluor 568. Confocal optical images (z section ~1 μm) were obtained from LV, septum (Sep), and right ventricle (RV). *B*: antibody labeling of RyR_2-$pSer^{2808}$ in control and isoproterenol (Iso)-treated heart. Scale bar, 2 μm. *C*: quantification of antibody labeling as fluorescence intensity (FI) in the optical section of the tissue. Background signal was very low (*top left*): FI values of all pixels were <34 (*top right*). Background signal was subtracted from each image before average optical density (OD) value was calculated (*bottom*). Scale bar, 20 μm. *D*: quantification of protein phosphorylation level. RyR_2-$pSer^{2808}$ and total RyR_2 were double labeled using a pair of phosphorylated epitope-specific and pan antibodies, each visualized using secondary antibody-conjugated Alexa Fluor 568 (red) and Alexa Fluor 488 (green), respectively. Ratio of phosphorylated to total RyR_2 optical density values was used to normalize RyR_2-$pSer^{2808}$ to total RyR_2. RyR_2-$pSer^{2808}$ labeling was more intense in failing heart from >1.5-yr-old SHR than >1.5-yr-old WKY; total RyR_2 labeling was comparable in >1.5-yr-old SHR and WKY. Scale bar, 20 μm. *E*: positive control. Control heart was infused with epinephrine (Epi). Labeling of RyR_2-$pSer^{2808}$ was more intense in epinephrine-treated than in control heart (*left*). Scale bar, 20 μm. Ratio of phosphorylated to total RyR_2 (P/T) from double-labeling experiment shows hyperphosphorylation in epinephrine-treated heart across ventricles (*right*; $n = 18$ tissue sections/group). $^*P < 0.05$; $^\wedge P < 0.1$. (Student's *t*-test). $P = 0.0007$ vs. control (2-way ANOVA). $P < 0.05$ for LV (posttest).

the heart caused β-adrenergic stimulation and increased PKA phosphorylation of RyR_2-Ser^{2808}.

The advantage of the SQ-IHC method is that it bypasses several protein-processing steps of the Western blot method, including tissue homogenization, protein extraction, total protein calibration, and protein transfer from gel to membrane, which should help reduce potential artifacts associated with these procedures. The disadvantage of the SQ-IHC method is

that molecular weights cannot be separated and very specific antibodies are required. Although we treated all samples using identical conditions throughout the antibody labeling and image acquisition procedures and employed the ratiometric method, the SQ-IHC measurement remains semiquantitative. However, the SQ-IHC method can be used in combination with Western blot to verify the data.

SQ-IHC measurement of RyR_2-Ser^{2808} phosphorylation. Sample images depicting double labeling of RyR_2-$pSer^{2808}$ and total RyR_2 in the SHR failing heart and age-matched WKY control are shown in Fig. 2*D*. Although total RyR_2 labeling (green) was comparable in SHR and WKY, RyR_2-$pSer^{2808}$ labeling (red) was more intense in SHR than WKY, demonstrating an increase in RyR_2-$pSer^{2808}$ relative to total RyR_2 in SHR.

Relative RyR_2-Ser^{2808} phosphorylation in various regions of the heart at three distinct stages of heart disease is shown in Fig. 3. In 11-wk-old SHR at the onset of hypertension before hypertrophy, RyR_2-$pSer^{2808}$ levels were similar to those in age-matched WKY across LV, septum, and right ventricle [RV; Fig. 3*A*; $P > 0.05$ for strain difference at each region (*t*-test) and $P > 0.05$ for strain difference across all regions (2-way ANOVA)]. In 1-yr-old SHR with overt cardiac hypertrophy, RyR_2-$pSer^{2808}$ remained normal in LV and septum but was significantly increased in RV [Fig. 3*B*; $P = 0.01$ for strain difference across all regions (2-way ANOVA) and $P < 0.05$ for RV (Bonferroni's posttest)]. In >1.5-yr-old SHR during HF, however, RyR_2-$pSer^{2808}$ was significantly increased across all regions of the heart, including LV, septum, and RV [Fig. 3*C*; $P = 0.002$ for strain difference across all regions (2-way ANOVA) and $P > 0.05$ possibly due to small sample numbers (Bonferroni's posttest)]. Interestingly, RyR_2-$pSer^{2808}$ was significantly higher in LV in >1.5-yr-old SHR ($P < 0.05$, *t*-test) but higher in RV 1-yr-old SHR [$P < 0.05$ (*t*-test) and $P < 0.05$ (Bonferroni's posttest)] than in age-matched WKY controls. Figure 3*D* shows the relative RyR_2-$pSer^{2808}$ levels in SHR normalized to age-matched WKY. The changes in LV measured using the SQ-IHC method are in agreement with those measure using Western blot (Fig. 1*C*).

SQ-IHC measurement of spatial distribution of RyR_2 clusters. The SQ-IHC method enabled us to measure not only the phosphorylation levels of RyR_2 but also the spatial localization of RyR_2 clusters (each contains ~100 RyR_2 molecules and serves as a CRU). We used a previously described method (7) (spatial resolution ~0.25 μm) to measure the longitudinal spacing between the neighboring RyR_2 clusters in the tissue cross sections (Fig. 4*A*). The histogram of CRU spacing showed a Gaussian distribution (Fig. 4*B*). The shorter CRU spacing in the failing heart of the SHR is manifested by a leftward shift of the distribution from that of WKY. To confirm the change of CRU spacing in the failing heart, we also used 2-mo-old healthy Sprague-Dawley rats as an additional control. As shown in Fig. 4*C*, CRU spacing is 1.72 ± 0.34 (SD) μm in the failing heart of the SHR, 9.5% shorter than in the age-matched WKY [1.90 ± 0.32 μm, $P < 0.01$ (*t*-test)] and 11.3% shorter than in the Sprague-Dawley control (1.94 ± 0.31 μm, $P < 0.01$). Since increased collagen expression in failing hearts (40) might constrain the cell length or shrink the tissue more on processing, we used collagenase and protease to enzymatically digest the heart to isolate ventricular myocytes. We conducted immunocytochemistry experiments to label

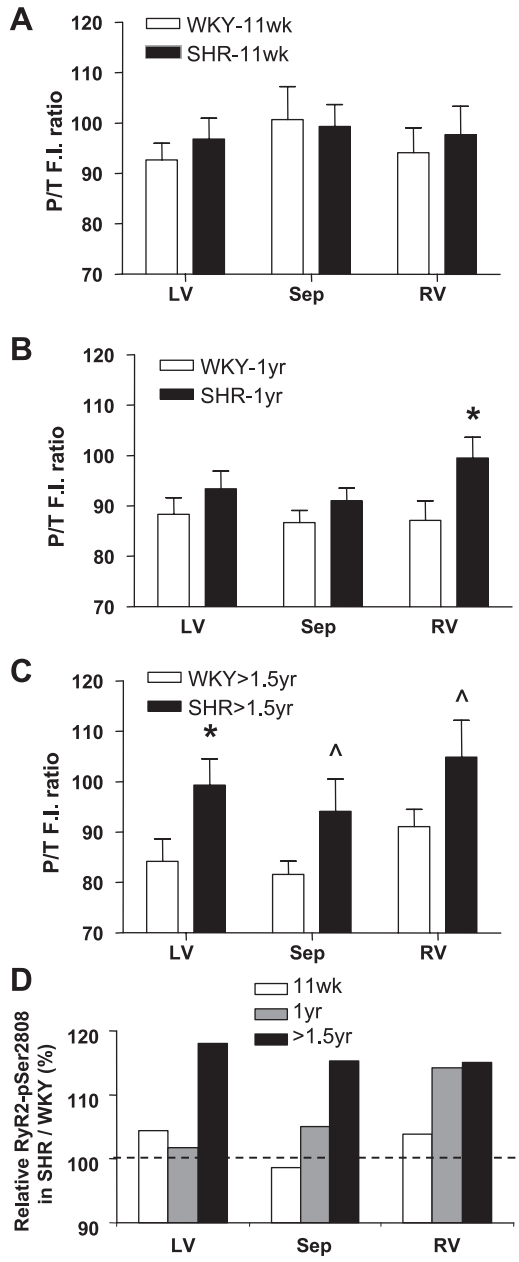

Fig. 3. Region-dependent changes in phosphorylation of RyR_2 during development of hypertensive heart disease. *A*: RyR_2-$pSer^{2808}$ normalized to total amount of RyR_2 in the LV, septum, and RV in WKY and SHR at 11 wk of age. At onset of hypertension before hypertrophy, RyR_2-$pSer^{2808}$ was similar in 11-wk-old SHR and WKY ($n = 9$ tissue sections/group). $P = 0.6$ for SHR vs. WKY (2-way ANOVA). *B*: RyR_2-$pSer^{2808}$ normalized to total amount of RyR_2 in LV, septum, and RV at 1 yr of age in WKY and SHR. In SHR with cardiac hypertrophy, RyR_2-$pSer^{2808}$ remained normal in LV and septum but increased in RV ($n = 9$ tissue sections/group). *$P < 0.05$ (Student's *t*-test). $P = 0.01$ for SHR vs. WKY (2-way ANOVA). $P < 0.05$ for RV (Bonferroni's posttest). *C*: RyR_2-$pSer^{2808}$ normalized to total amount of RyR_2 in LV, septum, and RV in 1.5-yr-old SHR and WKY. In SHR failing hearts, RyR_2-$pSer^{2808}$ became globally elevated across the ventricular section compared with WKY ($n = 9$ tissue sections/group). *$P < 0.05$; ^$P < 0.1$ (*t*-test). $P = 0.002$ for SHR vs. WKY across all regions (2-way ANOVA). $P > 0.05$ (Bonferroni's posttest). *D*: RyR_2-$pSer^{2808}$ in SHR normalized to age-matched WKY (ratio of mean values in SHR to WKY). RyR_2-$pSer^{2808}$ increased with disease development in LV, septum, and RV. Dashed line, WKY value used for normalization.

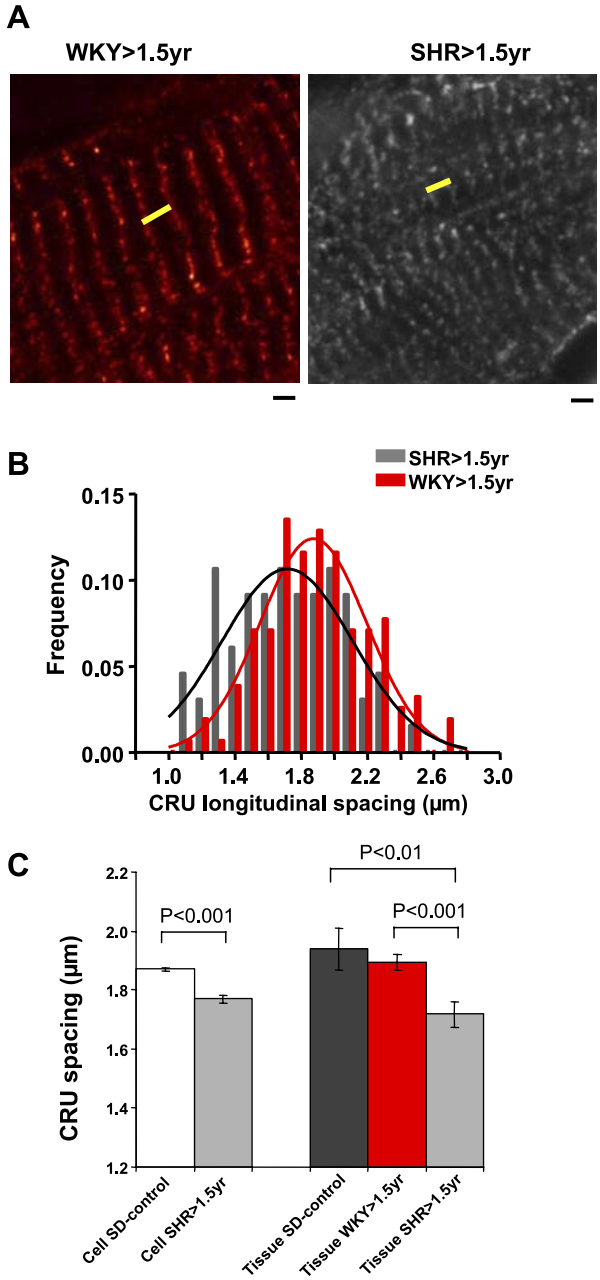

Fig. 4. Decreased spacing between RyR_2 Ca^{2+} release units (CRUs) in failing hearts of SHR. *A*: confocal images depicting representative RyR_2 labeling in tissue sections from SHR failing hearts and age-matched WKY control (pseudocolored red to distinguish from SHR). Yellow bars depict definition of CRU longitudinal spacing. Scale bars, 2 μm. *B*: normal distribution of CRU longitudinal spacing in SHR failing hearts ($n = 66$ determinants from 3 hearts) and WKY controls ($n = 156$ from 3 hearts). Distribution of spacing in SHR is leftward shifted from that of WKY: mean and variance from Gaussian fit of 1.72 ± 0.34 μm in SHR and 1.90 ± 0.32 μm in WKY ($P < 0.001$). *C*: CRU longitudinal spacing in isolated ventricular myocytes (cell) from Sprague-Dawley (SD) controls ($n = 786$ determinants) and SHR failing hearts ($n = 130$) and in tissue cross sections (tissue) from Sprague-Dawley ($n = 19$) and WKY controls ($n = 156$) and SHR failing hearts ($n = 66$). Values are means ± SD.

RyR_2 clusters in isolated cells and measured the longitudinal spacing between the antibody-labeled CRUs (Fig. 4*C*). Again, CRU spacing was shorter in cells from the failing heart of the SHR (1.77 ± 0.15, $n = 130$) than in cells from the Sprague-Dawley control [1.87 ± 0.18, $n = 786$, $P < 0.001$ (*t*-test)]. Furthermore, average CRU spacing in WKY and Sprague-Dawley control hearts is consistent with normal resting sarcomere length in ventricular myocytes (1.8–2.2 μm; data not shown), which demonstrates preserved cellular ultrastructure in the tissue section. (Since RyR_2 are localized in Z disks, the longitudinal spacing between CRUs corresponds to the sarcomere length.) Given that the identical protocol was used to prepare all tissues, the shorter CRU spacing in failing hearts of SHR cannot be attributed to artifacts that might change the cellular ultrastructure or to differential collagen expression. Therefore, it is most likely that shortening of the CRU longitudinal spacing in the failing heart is a real phenomenon of pathological significance.

DISCUSSION

Hyperphosphorylation of RyR_2-Ser^{2808} after progression from hypertrophy to HF in SHR. In the present study, we investigated two important factors that may contribute to changes in Ca^{2+} signaling during cardiac hypertrophy and HF: *1*) the phosphorylation status of the cardiac RyR (Ser^{2808}) and *2*) the spatial distribution of RyR_2 clusters within the cardiomyocytes. First, we conducted a longitudinal study to measure RyR_2-$pSer^{2808}$ in SHR at the four distinct stages in the development of hypertensive heart disease: prehypertension, hypertension before hypertrophy, cardiac hypertrophy, and finally HF. Western blot studies revealed that RyR_2-$pSer^{2808}$ in the LV of SHR was unaltered during the prehypertrophic and hypertrophic stages of hypertensive heart disease and became significantly elevated during HF. Immunohistochemistry studies further showed that RyR_2-$pSer^{2808}$ was normal during the prehypertrophic stage of hypertensive heart disease, whereas RyR_2-$pSer^{2808}$ became elevated in the RV of SHR with cardiac hypertrophy. After the development of overt HF in SHR, RyR_2-$pSer^{2808}$ significantly increased across the LV, septum, and RV in >1.5-yr-old rats. Overall, there was good agreement between the data obtained using Western blot and SQ-IHC. Hence, a major finding of this study is that hyperphosphorylation of RyR_2-Ser^{2808} occurs late during the development of hypertensive heart disease, after the development of cardiac failure.

Our data provide new insights into the controversy in the literature regarding increased phosphorylation of RyR_2-Ser^{2808} in structural heart disease. The finding that phosphorylation of RyR_2-Ser^{2808} is only increased in the LV of SHR with overt HF suggests that this posttranslational modification of the RyR may occur late during the development of HF. Our findings are consistent with enhanced PKA phosphorylation of RyR_2 in patients with end-stage HF (24, 31). Hyperphosphorylation of RyR_2 has also been reported in several animal models of HF, including a canine model of pacing-induced HF (30, 49), a rabbit aortic-banding model (1), and rat (26, 31) and mouse models of ischemic HF (45). Nonetheless, other studies found no changes in RyR_2-Ser^{2808} phosphorylation in patients and animals with HF. In light of the findings of our studies in SHR, it is likely that the degree of RyR_2-Ser^{2808} phosphorylation varies with the etiology and severity of heart disease. Indeed, Ward et al. (41) reported that SR Ca^{2+} load and RyR_2 function were not affected in SHR with mild symptoms of HF.

Factors that regulate RyR_2-Ser^{2808} phosphorylation: local control by kinases and phosphatases in the macromolecular complex. Phosphorylation of RyR_2-Ser^{2808} is regulated by multiple kinases and phosphatases in the RyR_2 macromolecular channel complex. Anchored via leucine/isoleucine zipper motifs on the cytoplasmic NH_2-terminal domain of RyR_2 are PKA [via its targeting protein, myocardial A kinase-anchoring protein (mAKAP)], Ca^{2+}-calmodulin-dependent protein kinase II (CaMKII), phosphatase PP1 (via protein spinophilin), phosphatase PP2A (via PR130), phosphodiesterase 4D3 (PDE4D3, via mAKAP), and several others, including calmodulin, FKBP12.6 (calstabin2), and sorcin (2, 18, 22, 24). Consequently, an increase in RyR_2-$pSer^{2808}$ could result from several events, e.g., increased PKA activity (31); downregulation of PDE4D3, which increases the local cAMP level and the PKA activity (18); or downregulation of PP1 and PP2A, which has been observed in patients with HF (24, 30, 32).

Furthermore, the RyR_2-Ser^{2808} phosphorylation site has been proposed to be a consensus phosphorylation site not only for PKA (RRXS), but also for CaMKII (RXXS) and PKG (RR/KXS/T) (16). Western blot experiments showed that RyR_2-Ser^{2808} could be phosphorylated, at least in vitro in SR vesicles or using purified RyR_2, by PKA and, possibly, by CaMKII (33, 47) or PKG (48). Using knock-in mice in which Ser^{2808} has been mutated to Ala, it has been demonstrated that Ser^{2808} is the major, physiologically active PKA phosphorylation site on RyR_2 (45). It remains to be seen whether CaMKII or PKG indeed phosphorylate RyR_2-Ser^{2808} in vivo. Finally, it has recently been suggested that Ser^{2030} on RyR_2 constitutes a second PKA phosphorylation site, although the physiological importance of this site remains controversial (48).

Functional consequences of RyR_2-Ser^{2808} phosphorylation: implications in HF. The functional consequences of PKA hyperphosphorylation of RyR_2 are the subject of scientific debate. Although PKA phosphorylation of RyR_2 increased the single RyR_2 channel activity in vitro in the planar lipid bilayers (24), the Ca^{2+} spark activity (each spark is generated by cooperative opening of a number of RyR_2 channels in a CRU) may not be changed by PKA phosphorylation in vivo (19). Plausible explanations for this controversy include *1*) incomplete PKA phosphorylation of RyR_2 in isolated cardiomyocytes and *2*) an increase in the opening of uncoupled RyR_2 channels ("rogue RyRs") by PKA phosphorylation of RyR_2 (36), which might cause small amounts of Ca^{2+} leak that could not be detected by the current technique.

It has been demonstrated that, in failing hearts, RyR_2 channels are more prone to abnormal SR Ca^{2+} release during diastole, leading to SR Ca^{2+} leak. One plausible explanation of enhanced SR Ca^{2+} release includes PKA hyperphosphorylation of RyR_2-Ser^{2808} (44). However, in failing rabbit hearts, SR Ca^{2+} leak could not be reduced using the PKA inhibitor H89 but was significantly blocked by CaMKII inhibition, suggesting that abnormal CaMKII phosphorylation of RyR_2 may also cause RyR_2 dysregulation in HF (1). Consistent with this notion, CaMKII phosphorylation of RyR_2 was shown to increase the Ca^{2+} spark activity in vivo (17, 13, 21), as well as the RyR_2 single-channel activity in vitro (46). Given that it has been proposed that CaMKII might also phosphorylate RyR_2-Ser^{2808} (33), the functional consequence of RyR_2-Ser^{2809} hyperphosphorylation (alone or in combination with other phosphorylation sites on RyR_2) remains to be determined.

Shortened RyR_2 cluster spacing is expected to promote spontaneous Ca^{2+} wave generation in the failing heart. It has been proposed that derangement of Ca^{2+} dynamics during HF could result not only from altered RyR_2 phosphorylation, but also from restructuring in the cellular organization that alters the coupling of RyR_2 with the neighboring RyR_2 or with other Ca^{2+}-handling molecules (14, 37). In failing hearts of SHR, spatial dispersion of the transverse t tubule system was found to disrupt the junctional coupling between CRUs and L-type Ca^{2+} channels, causing asynchronous Ca^{2+} spark activity (37). In a previous study, we predicted that the spatial distribution of RyR_2 clusters (CRUs) could also greatly affect Ca^{2+} wave generation (14). In the present study, we measured the distance between the RyR_2 clusters and found ~10% shortening of the CRU longitudinal spacing in failing hearts of SHR. This shortening of CRU spacing might be caused by several pathological factors in failing hearts. *1*) Elevated diastolic Ca^{2+} would cause impaired relaxation. *2*) Decreased phosphorylation levels of contractile proteins, including cardiac troponin I, troponin T, and myosin light chain 2, in SHR failing hearts (20) are expected to increase myofilament sensitivity to Ca^{2+} and, therefore, shorten sarcomere length and RyR_2 cluster longitudinal spacing (29, 38, 39). *3*) Increased collagen expression in failing hearts (40) might constrain the cell length or shrink the tissue more upon processing. However, experiments using cells enzymatically digested by collagenase and protease also showed shortening of the longitudinal CRU spacing in the cells from failing hearts. Hence, the CRU spacing change in the failing heart cannot be entirely attributed to collagen and is most likely caused by the elevated diastolic Ca^{2+} and increased myofilament sensitivity to Ca^{2+}.

Quantitative model simulations show that 10% shortening of CRU longitudinal spacing would greatly increase the probability of Ca^{2+} wave generation (14). Wave generation is further magnified when combined with an increased RyR_2 activity (14), and spontaneous Ca^{2+} waves are known to induce abnormal electrical activity and contribute to arrhythmias (for review see Ref. 5). In support of this scenario, increased arrhythmogenic activity has been associated with the development of cardiac hypertrophy and HF in SHR (10, 27, 28).

Summary. Our longitudinal study in rats with hypertensive heart disease provides new insights into the pathogenesis of abnormal Ca^{2+} handling in HF. In particular, our data demonstrate that phosphorylation of RyR_2-Ser^{2808} is increased only in SHR with end-stage HF. Moreover, our data suggest shortening of the spatial distance of CRUs in SHR failing hearts, which is expected to promote Ca^{2+}-induced Ca^{2+} release from neighboring CRUs (14) and contractile dysfunction. Additional studies are required to delineate the contribution of various modifications of RyR_2 and other Ca^{2+}-handling proteins during the development of hypertensive heart disease.

ACKNOWLEDGMENTS

We are grateful to Dr. Andrew R. Marks (Center for Molecular Cardiology, Columbia University) for kindly providing the phosphorylated epitope-specific antibody and Dr. Steven R. Reiken (Center for Molecular Cardiology, Columbia University) for help in performing Western blot experiments. We thank Drs. Robert J. Bloch and Jeanine A. Ursitti (Department of Physiology, University of Maryland) for kindly providing the cryostat and technical advice and Dr. Grace Sears for editing the manuscript.

GRANTS

This work was funded by American Heart Association National Scientist Development Grants 0335250N (Y. Chen-Izu) and 0535310N (X. H. T. Wehrens) and National Heart, Lung, and Blood Institute Grants K25 HL-068704 (L. T. Izu) and R01 HL-071865 (C. W. Balke and L. T. Izu).

REFERENCES

1. **Ai X, Curran JW, Shannon TR, Bers DM, Pogwizd SM.** Ca^{2+}/calmodulin-dependent protein kinase modulates cardiac ryanodine receptor phosphorylation and sarcoplasmic reticulum Ca^{2+} leak in heart failure. *Circ Res* 97: 1314–1322, 2005.
2. **Bers DM.** Macromolecular complexes regulating cardiac ryanodine receptor function. *J Mol Cell Cardiol* 37: 417–429, 2004.
3. **Bers DM, Eisner DA, Valdivia HH.** Sarcoplasmic reticulum Ca^{2+} and heart failure: roles of diastolic leak and Ca^{2+} transport. *Circ Res* 93: 487–490, 2003.
4. **Bing OH, Brooks WW, Robinson KG, Slawsky MT, Hayes JA, Litwin SE, Sen S, Conrad CH.** The spontaneously hypertensive rat as a model of the transition from compensated left ventricular hypertrophy to failure. *J Mol Cell Cardiol* 27: 383–396, 1995.
5. **Boyden PA, ter Keurs H.** Would modulation of intracellular Ca^{2+} be antiarrhythmic? *Pharmacol Ther* 108: 149–179, 2005.
6. **Brooks WW, Bing OH, Litwin SE, Conrad CH, Morgan JP.** Effects of treppe and calcium on intracellular calcium and function in the failing heart from the spontaneously hypertensive rat. *Hypertension* 24: 347–356, 1994.
7. **Chen-Izu Y, McCulle SL, Ward CW, Soeller C, Allen BM, Rabang C, Cannell MB, Balke CW, Izu LT.** Three-dimensional distribution of ryanodine receptor clusters in cardiac myocytes. *Biophys J* 91: 1–13, 2006.
8. **Conrad CH, Brooks WW, Robinson KG, Bing OH.** Impaired myocardial function in spontaneously hypertensive rats with heart failure. *Am J Physiol Heart Circ Physiol* 260: H136–H145, 1991.
9. **Drazner MH.** The transition from hypertrophy to failure: how certain are we? *Circulation* 112: 936–938, 2005.
10. **Evans SJ, Levi AJ, Jones JV.** Wall stress induced arrhythmia is enhanced by low potassium and early left ventricular hypertrophy in the working rat heart. *Cardiovasc Res* 29: 555–562, 1995.
11. **Frohlich ED.** Current issues in hypertension. Old questions with new answers and new questions. *Med Clin North Am* 76: 1043–1056, 1992.
12. **Gomez AM, Valdivia HH, Cheng H, Lederer MR, Santana LF, Cannell MB, McCune SA, Altschuld RA, Lederer WJ.** Defective excitation-contraction coupling in experimental cardiac hypertrophy and heart failure. *Science* 276: 800–806, 1997.
13. **Guo T, Zhang T, Mestril R, Bers DM.** Ca^{2+}/calmodulin-dependent protein kinase II phosphorylation of ryanodine receptor does affect calcium sparks in mouse ventricular myocytes. *Circ Res* 99: 398–406, 2006.
14. **Izu LT, Means SA, Shadid JN, Chen-Izu Y, Balke CW.** Interplay of ryanodine receptor distribution and calcium dynamics. *Biophys J* 91: 95–112, 2006.
15. **Jiang MT, Lokuta AJ, Farrell EF, Wolff MR, Haworth RA, Valdivia HH.** Abnormal Ca^{2+} release, but normal ryanodine receptors, in canine and human heart failure. *Circ Res* 91: 1015–1022, 2002.
16. **Kennelly PJ, Krebs EG.** Consensus sequences as substrate specificity determinants for protein kinases and protein phosphatases. *J Biol Chem* 266: 15555–15558, 1991.
17. **Kohlhaas M, Zhang T, Seidler T, Zibrova D, Dybkova N, Steen A, Wagner S, Chen L, Heller Brown J, Bers DM, Maier LS.** Increased sarcoplasmic reticulum calcium leak but unaltered contractility by acute CaMKII overexpression in isolated rabbit cardiac myocytes. *Circ Res* 98: 235–244, 2006.
18. **Lehnart SE, Wehrens XH, Reiken S, Warrier S, Belevych AE, Harvey RD, Richter W, Jin SL, Conti M, Marks AR.** Phosphodiesterase 4D deficiency in the ryanodine-receptor complex promotes heart failure and arrhythmias. *Cell* 123: 25–35, 2005.
19. **Li Y, Kranias EG, Mignery GA, Bers DM.** Protein kinase A phosphorylation of the ryanodine receptor does not affect calcium sparks in mouse ventricular myocytes. *Circ Res* 90: 309–316, 2002.
20. **Kaminsky M, Dike U, Afari-Armah N, Chen-Izu Y, Solaro RJ, Sumandea MP.** Differential phosphorylation of cTnT, cTnI and MLC2 with heart disease progression from pre-hypertension to heart failure. 2005 Biophysical Society Meeting Abstracts. *Biophysical Journal, Suppl,* 1542–Poster, 2005.
21. **Maier LS, Zhang T, Chen L, DeSantiago J, Brown JH, Bers DM.** Transgenic CaMKIIδC overexpression uniquely alters cardiac myocyte Ca^{2+} handling: reduced SR Ca^{2+} load and activated SR Ca^{2+} release. *Circ Res* 92: 904–911, 2003.
22. **Marks AR, Marx SO, Reiken S.** Regulation of ryanodine receptors via macromolecular complexes: a novel role for leucine/isoleucine zippers. *Trends Cardiovasc Med* 12: 166–170, 2002.
23. **Marks AR, Reiken S, Marx SO.** Progression of heart failure: is protein kinase A hyperphosphorylation of the ryanodine receptor a contributing factor? *Circulation* 105: 272–275, 2002.
24. **Marx SO, Reiken S, Hisamatsu Y, Jayaraman T, Burkhoff D, Rosemblit N, Marks AR.** PKA phosphorylation dissociates FKBP12.6 from the calcium release channel (ryanodine receptor): defective regulation in failing hearts. *Cell* 101: 365–376, 2000.
25. **Matkowskyj KA, Cox R, Jensen RT, Benya RV.** Quantitative immunohistochemistry by measuring cumulative signal strength accurately measures receptor number. *J Histochem Cytochem* 51: 205–214, 2003.
26. **Obayashi M, Xiao B, Stuyvers BD, Davidoff AW, Mei J, Chen SRW, ter Keurs HEDJ.** Spontaneous diastolic contractions and phosphorylation of the cardiac ryanodine receptor at serine-2808 in congestive heart failure in rat. *Cardiovasc Res* 69: 140–151, 2006.
27. **Pahor M, Bernabei R, Sgadari A, Gambassi G Jr, Lo Giudice P, Pacifici L, Ramacci MT, Lagrasta C, Olivetti G, Carbonin P.** Enalapril prevents cardiac fibrosis and arrhythmias in hypertensive rats. *Hypertension* 18: 148–157, 1991.
28. **Pahor MLGP, Bernabei R, Di Gennaro M, Pacifici L, Ramacci MT, Carbonin PU.** Age-related increase in the incidence of ventricular arrhythmias in isolated hearts from spontaneously hypertensive rats. *Cardiovasc Drugs Ther* 3: 163–169, 1989.
29. **Pyle WG, Sumandea MP, Solaro RJ, de Tombe PP.** Troponin I serines 43/45 and regulation of cardiac myofilament function. *Am J Physiol Heart Circ Physiol* 283: H1215–H1224, 2002.
30. **Reiken S, Gaburjakova M, Gaburjakova J, He KL, Prieto A, Becker E, Yi GH, Wang J, Burkhoff D, Marks AR.** β-Adrenergic receptor blockers restore cardiac calcium release channel (ryanodine receptor) structure and function in heart failure. *Circulation* 104: 2843–2848, 2001.
31. **Reiken S, Gaburjakova M, Guatimosim S, Gomez AM, D'Armiento J, Burkhoff D, Wang J, Vassort G, Lederer WJ, Marks AR.** Protein kinase A phosphorylation of the cardiac calcium release channel (ryanodine receptor) in normal and failing hearts. Role of phosphatases and response to isoproterenol. *J Biol Chem* 278: 444–453, 2003.
32. **Reiken S, Wehrens XH, Vest JA, Barbone A, Klotz S, Mancini D, Burkhoff D, Marks AR.** β-Blockers restore calcium release channel function and improve cardiac muscle performance in human heart failure. *Circulation* 107: 2459–2466, 2003.
33. **Rodriguez P, Bhogal MS, Colyer J.** Stoichiometric phosphorylation of cardiac ryanodine receptor on serine 2809 by calmodulin-dependent kinase II and protein kinase A. *J Biol Chem* 278: 38593–38600, 2003.
34. **Rysa J, Leskinen H, Ilves M, Ruskoaho H.** Distinct upregulation of extracellular matrix genes in transition from hypertrophy to hypertensive heart failure. *Hypertension* 45: 927–933, 2005.
35. **Slama M, Ahn J, Varagic J, Susic D, Frohlich ED.** Long-term left ventricular echocardiographic follow-up of SHR and WKY rats: effects of hypertension and age. *Am J Physiol Heart Circ Physiol* 286: H181–H185, 2004.
36. **Sobie EA, Guatimosim S, Gomez-Viquez L, Song LS, Hartmann H, Saleet Jafri M, Lederer WJ.** The Ca^{2+} leak paradox and "rogue ryanodine receptors": SR Ca^{2+} efflux theory and practice. *Prog Biophys Mol Biol* 90: 172–185, 2006.
37. **Song LS, Sobie EA, McCulle S, Lederer WJ, Balke CW, Cheng H.** Orphaned ryanodine receptors in the failing heart. *Proc Natl Acad Sci USA* 103: 4305–4310, 2006.
38. **Sumandea MP, Pyle WG, Kobayashi T, de Tombe PP, Solaro RJ.** Identification of a functionally critical protein kinase C phosphorylation residue of cardiac troponin T. *J Biol Chem* 278: 35135–35144, 2003.
39. **Van der Velden J, Papp Z, Zaremba R, Boontje NM, de Jong JW, Owen VJ, Burton PBJ, Goldmann P, Jaquet K, Stienen GJM.** Increased Ca^{2+}-sensitivity of the contractile apparatus in end-stage human heart failure results from altered phosphorylation of contractile proteins. *Cardiovasc Res* 57: 37–47, 2003.
40. **Venetucci L, Trafford AW, Eisner DA.** Illuminating sarcoplasmic reticulum calcium. *Circ Res* 93: 4–5, 2003.

41. **Ward ML, Pope AJ, Loiselle DS, Cannell MB.** Reduced contraction strength with increased intracellular [Ca^{2+}] in left ventricular trabeculae from failing rat hearts. *J Physiol* 546: 537–550, 2003.
42. **Wehrens XH, Lehnart SE, Huang F, Vest JA, Reiken SR, Mohler PJ, Sun J, Guatimosim S, Song LS, Rosemblit N, D'Armiento JM, Napolitano C, Memmi M, Priori SG, Lederer WJ, Marks AR.** FKBP12.6 deficiency and defective calcium release channel (ryanodine receptor) function linked to exercise-induced sudden cardiac death. *Cell* 113: 829–840, 2003.
43. **Wehrens XH, Lehnart SE, Marks AR.** Intracellular calcium release and cardiac disease. *Annu Rev Physiol* 67: 69–98, 2005.
44. **Wehrens XH, Lehnart SE, Reiken S, van der Nagel R, Morales R, Sun J, Cheng Z, Deng SX, de Windt LJ, Landry DW, Marks AR.** Enhancing calstabin binding to ryanodine receptors improves cardiac and skeletal muscle function in heart failure. *Proc Natl Acad Sci USA* 102: 9607–9612, 2005.
45. **Wehrens XH, Lehnart SE, Reiken S, Vest JA, Wronska A, Marks AR.** Ryanodine receptor/calcium release channel PKA phosphorylation: a critical mediator of heart failure progression. *Proc Natl Acad Sci USA* 103: 511–518, 2006.
46. **Wehrens XHT, Lehnart SE, Reiken SR, Marks AR.** Ca^{2+}/calmodulin-dependent protein kinase II phosphorylation regulates the cardiac ryanodine receptor. *Circ Res* 94: e61–e70, 2004.
47. **Witcher DR, Kovacs RJ, Schulman H, Cefali DC, Jones LR.** Unique phosphorylation site on the cardiac ryanodine receptor regulates calcium channel activity. *J Biol Chem* 266: 11144–11152, 1991.
48. **Xiao B, Zhong G, Obayashi M, Yang D, Chen K, Walsh MP, Shimoni Y, Cheng H, Ter Keurs H, Chen SR.** Ser-2030, but not Ser-2808, is the major phosphorylation site in cardiac ryanodine receptors responding to protein kinase A activation upon β-adrenergic stimulation in normal and failing hearts. *Biochem J* 396: 7–16, 2006.
49. **Yano M, Kobayashi S, Kohno M, Doi M, Tokuhisa T, Okuda S, Suetsugu M, Hisaoka T, Obayashi M, Ohkusa T, Kohno M, Matsuzaki M.** FKBP12.6-mediated stabilization of calcium-release channel (ryanodine receptor) as a novel therapeutic strategy against heart failure. *Circulation* 107: 477–484, 2003.